phys. stat. sol. (b) **241**, No. 12, 2839–2842 (2004) / **DOI** 10.1002/pssb.200405049

Epitaxial growth of hexagonal and cubic InN films

K. Nishida[*, 1], **Y. Kitamura**[1], **Y. Hijikata**[1, 2], **H. Yaguchi**[1, 2], and **S. Yoshida**[1, 2]

[1] Department of Electrical and Electronic Systems Engineering, Faculty of Engineering, Saitama University, 255 Shimo-Ohkubo, Sakura-ku, Saitama-shi, 338-8570, Japan
[2] CREST, JST, 4-1-8 Hon-cho, Kawaguchi-shi, Saitama, 332-0012, Japan

Received 23 June 2004, accepted 5 July 2004
Published online 2 September 2004

PACS 81.05.Ea, 81.15.Hi

We have grown InN films on 3C-SiC (001) substrates with and without cubic GaN underlayers by RF-N_2 plasma MBE. It was found that, in the case of direct growth on 3C-SiC (001), hexagonal InN grows with the crystal orientation as hexagonal InN $(1\bar{1}00)$//3C-SiC (110), while, in the case of the growth on cubic GaN underlayers, cubic InN grows with the crystal orientation as cubic InN (110)//cubic GaN (110). Photoluminescence emissions from the cubic and hexagonal InN films were clearly observed at around 0.7 eV.

1 Introduction

It is well known that group III nitrides have hexagonal wurtzite crystal structure, differing from other III–V compounds which usually crystallize in the cubic zincblende structure. However, cubic III nitrides can be obtained when (001) surfaces of cubic crystals, such as GaAs and 3C-SiC, are used as substrates. It has been expected that cubic nitrides have some advantages for optical and electrical device applications compared with hexagonal ones, including higher carrier mobility due to less lattice scattering, better doping properties and superior optical properties [1]. Cubic GaN, AlN and their alloy films have been grown on GaAs, 3C-SiC, Si and MgO by MBE and MOCVD and their physical properties, including their bandgap energies, have been reported by many authors [2, 3]. It has recently been reported on the results of *ab initio* calculations of the bandgap energies of hexagonal and cubic InN as 0.81 and 0.58 eV, respectively [4]. Cubic InN films have been reported to grow on GaAs (001) substrates with InAs underlayers [5] and on r-plane sapphire substrates [6]. However, little has been reported on the crystal qualities of grown cubic InN films and their physical properties. In this paper, we report on the epitaxial growth of InN films on 3C-SiC (001) substrates with and without cubic GaN (c-GaN) underlayers and discuss on the growth conditions of c- and hexagonal InN (h-InN) films. We also report on the luminescent properties of the InN films obtained.

2 Experimental procedures

We have grown InN films on 3C-SiC (001) substrates by gas source MBE using a RF-N_2 plasma source. 3C-SiC (001) epilayers were obtained by CVD growth on Si (001) substrates at around 1300 °C. Details of the growth of 3C-SiC on Si have been described elsewhere [7]. We have tried to grow InN films with and without c-GaN underlayers. In the former case, prior to the growth of InN, c-GaN epilayers, around 0.5 μm in thickness, were grown on 3C-SiC at 760 °C. The hexagonal GaN phase content of the epilayers was around 2–3%, and c-GaN single crystal films grow with the crystal orientation parallel to that of

[*] Corresponding author: e-mail: kenji-n@opt.ees.saitama-u.ac.jp, Tel/Fax: +81-48-858-3470

3C-SiC. InN buffer layers were grown at 300 °C for 2 min directly on 3C-SiC or on c-GaN underlayers. After the growth of buffer layers, the substrates were heated up to 400–550 °C, and then InN films were grown for 1 hour. The crystal structures were monitored during growth by use of reflection high-energy electron diffraction (RHEED). We have studied the crystal structures and morphologies by X-ray diffraction (XRD) and scanning electron microscope (SEM), respectively. We have measured photoluminescence (PL) spectra of the InN films at 5 K using the 633 nm line of a He-Ne laser.

3 Results and discussion

3.1 Direct growth on 3C-SiC substrates

We have grown InN films directly on 3C-SiC (001) substrates. The thicknesses of the films were around 0.3 μm for 1-hour growth. SEM observation revealed that the surfaces were almost smooth, but sometimes had round pits. RHEED patterns showed a streak feature during and after the InN growth. The interval of the streak lines was almost unchanged by the growth of InN films. An XRD pattern (θ–2θ scan) for an InN film directly grown on 3C-SiC at 550 °C is shown in Fig. 1(a). The diffraction peak assigned to h-InN (0002) is seen as well as that from 3C-SiC substrate, and no peak assigned to cubic phase is seen at all. Fig. 1(b) shows XRD ϕ scan patterns for asymmetric h-InN $\{1\bar{1}02\}$ and 3C-SiC $\{111\}$ planes. The diffraction pattern for hexagonal InN $\{1\bar{1}02\}$ show peaks at every 60°, i.e., 6-fold symmetry and the peaks for hexagonal InN $\{1\bar{1}02\}$ coincide with those for 3C-SiC $\{111\}$ every 180°. These results, as well as those of RHEED observation, suggest that in the case of the direct growth on 3C-SiC, h-InN grows with the crystal orientation as h-InN $(1\bar{1}00)$//3C-SiC (110), and h-InN films grown on 3C-SiC (001) do not show double positioning, but are composed of single domain. The full widths at half maximum (FWHM) of XRD rocking curve for h-InN (0002) peak were around 15 arcmin. We have tried to grow c-InN directly on 3C-SiC (001) substrates with various growth conditions. However, we have failed to obtained c-InN directly on 3C-SiC (001) substrates.

The lattice mismatch between 3C-SiC (001)/c-InN (001) is calculated as 14%, which is much larger than that in the case of 3C-SiC/c-GaN, i.e., 3.8%. On the contrary, the lattice mismatch between 3C-SiC (110) and h-InN $(1\bar{1}00)$ is as small as 0.3%, which can explain the experimental results that the interval of the streak lines was almost unchanged by the growth of InN films. These may result in the preferential growth of not cubic but hexagonal InN on 3C-SiC (001) substrates. It was found that the preferential crystal orientation of h-InN on 3C-SiC has not 12-fold symmetry but 6-fold symmetry for the axis normal to the substrate surface. We can explain this by the consideration that 3C-SiC has zincblende structure and the 3C-SiC substrates we used are composed of single domain, which means the crystal symmetry is not 4-fold but 2-fold [7].

3.2 Growth on cubic GaN underlayers

We have grown InN films on 3C-SiC with c-GaN underlayers. First, c-GaN films were epitaxially grown at 760 °C, around 0.5 μm in thickness, on 3C-SiC (001) substrates. Subsequently, InN films were grown

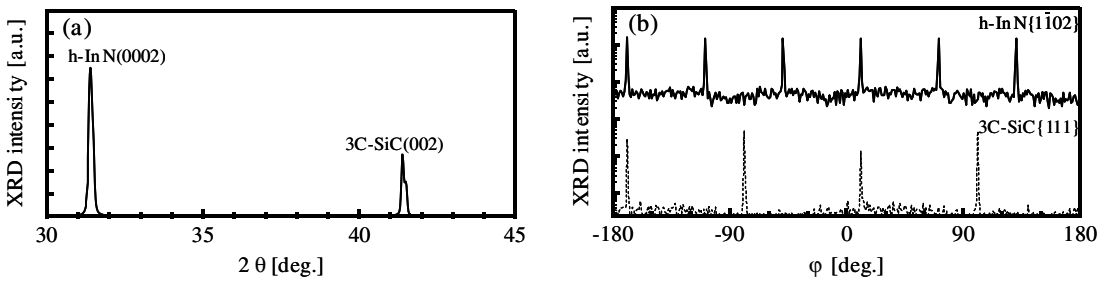

Fig. 1 X-ray diffraction patterns from an InN film grown directly on 3C-SiC (001); (a) θ–2θ scan and (b) ϕ scan. The Solid and dotted lines in (b) are diffraction patterns for asymmetric hexagonal InN $\{1\bar{1}02\}$ and 3C-SiC $\{111\}$, respectively.

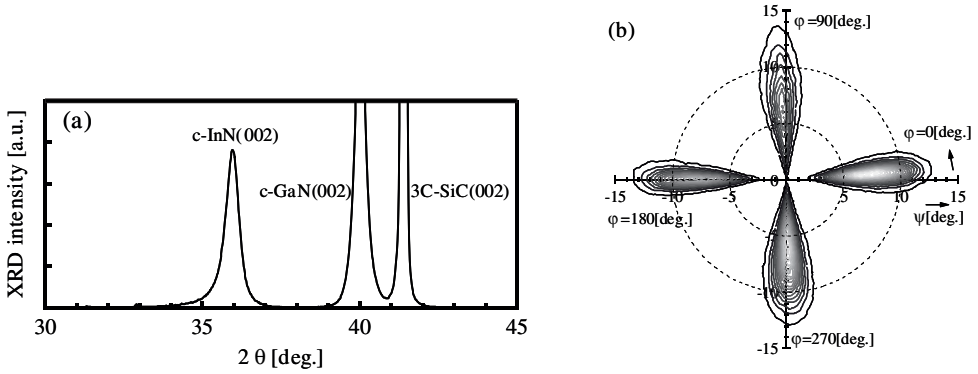

Fig. 2 X-ray diffraction patterns from an InN film grown on a cubic GaN underlayer; (a) θ–2θ scan and (b) pole figure for h-InN $(1\bar{1}01)$ diffraction condition.

on the c-GaN underlayers for 1 hour. RHEED patterns changed from streak c-GaN patterns to spotty c-InN patterns. RHEED observation suggests that c-InN single crystal films grow with the crystal orientation parallel to that of c-GaN in the case of the growth on c-GaN underlayers.

An XRD pattern (θ–2θ scan) for an InN film on a c-GaN underlayer is shown in Fig. 2(a). Only the diffraction peak assigned to c-InN (002) is seen, and no peak assigned to hexagonal phase is seen. The XRD measurements also suggest that c-InN films grow on c-GaN underlayer. Figure 2(b) shows the XRD pole figure for h-InN $(1\bar{1}01)$ Bragg diffraction conditions of an InN film grown on c-GaN underlayer. The figure suggests that *c*-axis of h-InN crystals contained in the film are parallel to the $\langle 111 \rangle$ axis of c-InN crystals.

It has been reported that the comparison of the XRD peak intensity for c-GaN (002) with that for h-GaN $(1\bar{1}01)$ is useful for estimating the h-GaN phase content of c-GaN films [8]. However, in the case of InN, it is difficult to use the XRD peak intensity for h-InN $(1\bar{1}01)$ to estimate the hexagonal phase content of the films correctly, since the lattice plane spacing of h-InN $(1\bar{1}01)$ is almost the same as those of Si (002) and In (101). Therefore, we have estimated the hexagonal phase content of the films from the XRD intensity ratio of the peaks for c-InN (002) and h-InN $(1\bar{1}02)$. In the calculation of the content, we have taken into account that the XRD scattering factor for c-InN (002) is 3.5 times as that for h-InN $(1\bar{1}02)$. The hexagonal phase contents of the InN films grown on c-GaN underlayers at 400 °C, 440 °C, 450 °C and 500 °C, the thicknesses of which were around 0.44 μm, were estimated to be 84%, 42%, 35% and 90%, respectively. The FWHM of XRD rocking curve for c-InN (002) was 76 arcmin.

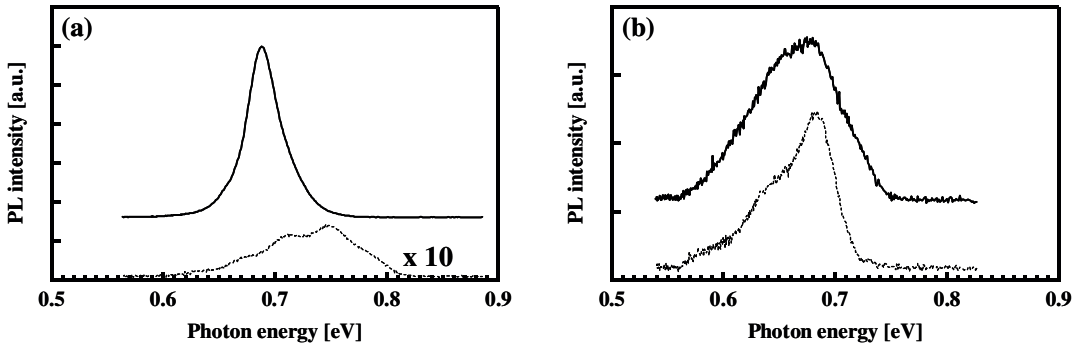

Fig. 3 Photoluminescence spectra for InN films grown (a) directly on 3C-SiC (001) at 550 °C (solid line) and 470 °C (dotted line), and (b) on cubic GaN underlayers at 450 °C (solid line) and 440 °C (dotted line). The measurements were performed at 5 K.

3.3 PL measurements of cubic and hexagonal InN films

Low temperature PL spectra of InN films grown directly on 3C-SiC at 470 °C and 550 °C, and those on c-GaN underlayers at 440 °C and 450 °C, the hexagonal phase content of which are lower compared with the films grown at other temperatures, are shown in Figs. 3(a) and (b). All the InN films measured show a peak at around 0.7 eV. Especially, the h-InN film grown at 550 °C shows a very sharp peak at 0.69 eV. Although the PL peaks in c-InN films are observed at somewhat lower energies than those in h-InN, the effects of the Burstein-Moss shift and hexagonal phase contained in c-InN films have to be taken into account in order to discuss the difference in the bandgap energies between c- and h-InN from PL spectra.

4 Conclusion

We have successfully grown cubic and hexagonal InN films on 3C-SiC (001) substrates with and without c-GaN underlayers by RF-N_2 plasma MBE, respectively. In the case of the direct growth on 3C-SiC (001), h-InN grows with the crystal orientation as h-InN $(1\bar{1}00)$//3C-SiC (110) while, in the case of the growth on c-GaN underlayers, c-InN grows with the crystal orientation as c-InN (110)//c-GaN (110). PL emission was clearly observed at around 0.7 eV from c- and h-InN films obtained. To discuss the difference in the bandgap energies between c- and h-InN, further studies on the electrical properties of InN films are required as well as the efforts to reduce the hexagonal phase content of c-InN films.

Acknowledgements The authors would like to thank Y. Ishida and T. Takahashi of AIST and T. Kitamura of Tokyo University of Science for supplying 3C-SiC substrates. XRD and PL measurements were carried out at the University of Tokyo. We are grateful to S. Koh and R. Katayama for their support.

References

[1] S. Yoshida, Physica E **7**, 907 (2000).
[2] H. Okumura, K. Ohto, G. Feuillet, K. Balakrishnan, S. Chichibu, H. Hamaguchi, P. Hacke, and S. Yoshida, J. Cryst. Growth **178**, 113 (1997).
[3] T. Suzuki, H. Yaguchi, H. Okumura, Y. Ishida, and S. Yoshida, Jpn. J. Appl. Phys. **39**, L497 (2000).
[4] F. Bechstedt, J. Furthmüller, M. Ferhat, L. K. Teles, L. M. R. Scolfaro, J. R. Leite, V. Y. Davydov, O. Ambacher, and R. Goldhahn, phys. stat. sol. (a) **195**(3), 628 (2003).
[5] A. P. Lima, A. Tabata, J. R. Leite, S. Kaiser, D. Schikora, B. Schöttker, T. Frey, D. J. As, and K. Lischka, J. Cryst. Growth **201/202**, 396 (1999).
[6] V. Cimalla, J. Pezoldt, G. Ecke, R. Koshiba, O. Ambacher, L. Spieß, G. Teichert, H. Lu, and W. J. Schaff, Appl. Phys. Lett. **83**, 27 (2003).
[7] Y. Ishida, T. Takahashi, H. Okumura, S. Yoshida, and T. Sekigawa, Jpn. J. Appl. Phys. **36**, 6633 (1997).
[8] H. Tsuchiya, K. Sunaba, S. Yonemura, T. Suemasu, and F. Hasegawa, Jpn. J. Appl. Phys. **36**, L1 (1997).